

Diffractive energy spreading and its semiclassical limit

Alexander Stotland and Doron Cohen

Department of Physics, Ben-Gurion University, Beer-Sheva 84005, Israel

Received 24 May 2006, in final form 17 July 2006

Published 9 August 2006

Online at stacks.iop.org/JPhysA/39/10703

Abstract

We consider driven systems where the driving induces jumps in energy space: (1) particles pulsed by a step potential; (2) particles in a box with a moving wall; (3) particles in a ring driven by an electro-motive-force. In all these cases, the route towards quantum-classical correspondence is highly non-trivial. Some insight is gained by observing that the dynamics in energy space, where n is the level index, is essentially the same as that of Bloch electrons in a tight binding model, where n is the site index. The mean level spacing is like a constant electric field and the driving induces long range hopping $\propto 1/(n - m)$.

PACS numbers: 03.65.-w, 03.65.Sq, 05.45.Mt

(Some figures in this article are in colour only in the electronic version)

1. Introduction

Consider a system which is described by a Hamiltonian $\mathcal{H}(X(t))$, where the parameter $X(t)$ is time dependent. For such a system the energy E is not a constant of the motion. Rather, the driving induces spreading in energy space. Assuming that the system is prepared at $t = 0$ in a microcanonical state, one wonders how the energy distribution $\rho_t(E)$ looks like at a later time. In particular, one may wonder whether the quantum $\rho_t(E)$ is similar to the corresponding classical distribution. In the ‘quantum chaos’ literature it is customary to distinguish between a classical time scale τ_{cl} and a quantum brektime t^* . The latter goes to infinity in the ‘ $\hbar \rightarrow 0$ ’ limit. A prototype model is the ‘quantum kicked rotator’ [1] where the energy spreading is diffusive up to t^* , while for larger times one observes saturation due to a dynamical localization effect.

In this work, we analyse much simpler systems where the brektime t^* , if exists, is much larger than any physically relevant time scale. In fact, one may assume that the time t of the evolution is comparable with the classical (short) time scale. In such circumstances, one naively would expect quantum to classical correspondence (QCC). But in fact the theory is much more complicated [2]. One has to distinguish between

- detailed QCC and
- restricted QCC.

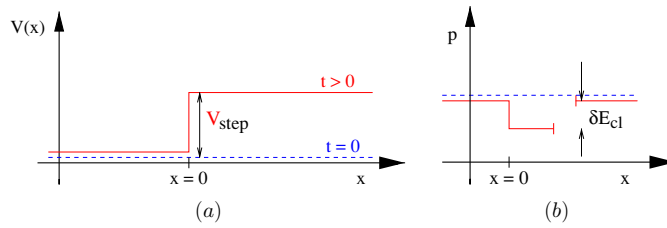


Figure 1. (a) Left panel: picture of the potential. Before $t = 0$ the potential is zero (dashed line). After $t = 0$ the potential is the step function (solid line). (b) Right panel: phase space picture. Before $t = 0$ there is no potential and the momentum is constant (dashed line). The piece of the distribution that has passed $x = 0$ after $t = 0$ is boosted with $\delta E_{cl} = -V_{step}$.

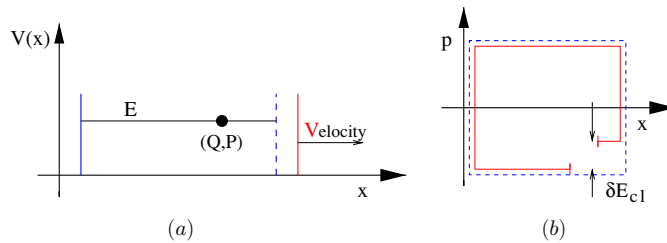


Figure 2. (a) Left panel: potential well. The right wall is moving with a constant velocity V_{wall} . (b) Right panel: phase space picture. If the wall were not moving, the distribution would evolve along the dashed line. If V_{wall} is non-zero, an energy jump $\delta E_{cl} = -2mv_E V_{wall}$ is associated with the collision, and one obtains the distribution which is illustrated by the solid line.

Detailed QCC means that all the moments $r = 1, 2, 3, \dots$ of the quantum mechanical distribution $\rho_t(E)$ are similar to the classical result, while restricted QCC refers only to the $r = 1, 2$ moments. It turns out that the latter are very robust, while the higher moments ($r > 2$) might be much larger in the quantum case. Our first challenge would be to find and to analyse the *worst case* for QCC, for which all the $r > 2$ moments are classically finite but quantum mechanically divergent. We would like to see whether in such circumstances restricted QCC for $r = 1, 2$ survives.

For completeness of this introduction, we summarize in appendix A the reason for the robustness of restricted QCC. Our interest in QCC is motivated by the wish to develop a better understanding of driven systems. We would like to explore examples where QCC is far from obvious even for short times. In what follows, we address four problems that in first sight look unrelated:

- (1) Particles that are pulsed by a step potential (figure 1).
- (2) Particles in a box with a moving wall (figure 2).
- (3) Particles in an electro-motive-force (EMF) driven ring (figure 3).
- (4) Wavepacket dynamics of Bloch electrons in a constant electric field.

In fact, we are going to see that problems (1)–(3) share a common feature: in the classical description the energy absorption is associated with abrupt *jumps* in phase space. These jumps are reflected in the quantum dynamics as a strong *diffraction* effect. This diffraction, which takes place in energy space, is the worst case for Bohr's QCC. It turns out that problem (1) can be solved exactly, while problems (2) and (3) reduce essentially to problem (4). Namely, the

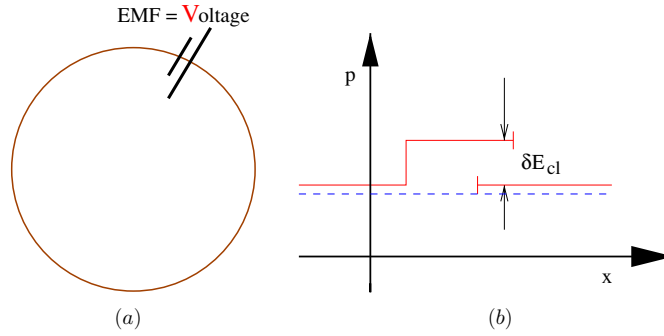


Figure 3. (a) Left panel: ring with EMF. (b) Right panel: phase space picture. Without the EMF the momentum is a constant of the motion (dashed line). Else an energy jump $\delta E_{cl} = eV_{EMF}$ is associated with each crossing of the EMF step. The emerging phase space distribution is illustrated by the solid line.

dynamics in energy space, where n is the level index, is essentially the same as that of Bloch electrons in a tight binding model, where n is the site index. The mean level spacing is like a constant electric field and the driving induces long range hopping $\propto 1/(n - m)$. This tight binding problem has an exact solution. The objectives of the present work are as follows:

- To highlight the route towards QCC in the case of diffractive energy spreading.
- To provide solutions and numerical demonstrations to the prototype problems.
- To shed new light of the EMF-driven ring problem.
- To illuminate the limitations of linear response theory in the mesoscopic context.

The paper is structured accordingly.

A few words are in order regarding the literature. The quantum treatment of the ‘moving wall’ problem has started with [3, 4] that were aimed in finding the steady-state solutions for an expanding well. The interest in this model has further evolved within the study of the Fermi acceleration problem [5] where the wall is oscillating. Recently, the non-trivial features of the parametric [6] and of the time-dependent wavepacket dynamics [7] were illuminated. In the latter publication, a satisfactory mathematical treatment of the non-stationary dynamics has not been introduced. Also the problem of Bloch electrons in a constant electric field has a long history. The concept of a Stark ladder was introduced by Wannier [8] to describe the energy spectrum of a periodic system in an electric field. Since that time it has become the subject of controversy [9–19]. Eventually, it has been realized that the electric field localizes the motion of the electrons and induces a periodic oscillatory motion.

2. Energy jumps in phase space

If a Gaussian wavepacket is moving in a smooth potential, then its Wigner function evolves in a smooth manner which favours detailed QCC. But we would like to consider the ‘worst case’ for QCC. Let us assume that the particle is prepared with some initial momentum p . This means in practice a very extended wavepacket with a very small dispersion in momentum. We turn on at $t = 0$ a step of height V_{step} . After a short time t , we observe that the classical phase space distribution is torn into three pieces (see figure 1): phase space points that remain on the left side of the step; phase space points that have crossed the step from left to right and

phase space points that were all the time in the right side of the step. The jump in the kinetic energy of those points that have crossed the step is

$$\delta E_{\text{cl}} = -V_{\text{step}}. \quad (1)$$

Classically we have in phase space points that move with the original kinetic energy, and another set of points that have gone through an abrupt change of kinetic energy. Thus, the energy distribution consists of two delta peaks. We would like to know what is the corresponding energy distribution in the quantum mechanical case.

A similar phase space picture emerges in the analysis of the ‘moving wall’ problem. As illustrated in figure 2, we have a particle of mass m and energy E bouncing back and forth inside a one-dimensional box. One wall of the box is displaced with a velocity V_{wall} , which is assumed to be much smaller compared with the velocity $v_E = (2E/m)^{1/2}$ of the bouncing particle. Consider an initial microcanonical distribution. After a short time t , some of the phase space points collide with the wall which is moving with velocity V_{wall} . Consequently, their velocity undergoes a change $v \mapsto -v + 2V_{\text{wall}}$, and accordingly the energy jump is

$$\delta E_{\text{cl}} = -2mv_E V_{\text{wall}}. \quad (2)$$

Thus, after a short time the energy distribution consists of two delta peaks: one corresponds to those phase space points that did not collide with the moving wall and the other corresponds to those phase space points that did collide with the moving wall. We ask what is the corresponding quantum result. Namely, how the probability is distributed among the energy levels in the quantum mechanical case. It is implicit that we are going to work in the adiabatic (wall location dependent) basis, else the question is mathematically ill defined.

Possibly the most interesting and experimentally relevant model is that of a one-dimensional EMF-driven ring (figure 3). The classical analysis for this problem is very simple: each time that the particle crosses the EMF step its energy changes by

$$\delta E_{\text{cl}} = eV_{\text{EMF}}. \quad (3)$$

So also here we have energy jumps. Surprisingly, this problem is interesting even if we do not add a scatterer.

3. Beyond the Fermi golden rule, the semiclassical regime

Both in the case of the ‘moving wall’ and in the case of the driven ring we have after a short time a finite probability to find the system with a different energy. So, we may say that there is some finite probability to make a transition

$$E \mapsto E + \delta E_{\text{cl}}. \quad (4)$$

Going to the quantum mechanical problem, we may wonder whether or how we get from the Schrödinger equation such transitions. We are used to the Fermi golden rule picture of transitions

$$E \mapsto E + \hbar\omega \quad (5)$$

where ω is the frequency of the driving. But here we do not have periodic (‘ac’) driving but rather linear (‘dc’) driving. Moreover, δE_{cl} is an \hbar -independent quantity. It turns out that indeed there exists a regime where the dynamics is classical like (figure 4). This semiclassical regime is defined by the obvious condition

$$\delta E_{\text{cl}} \gg \Delta \quad (6)$$

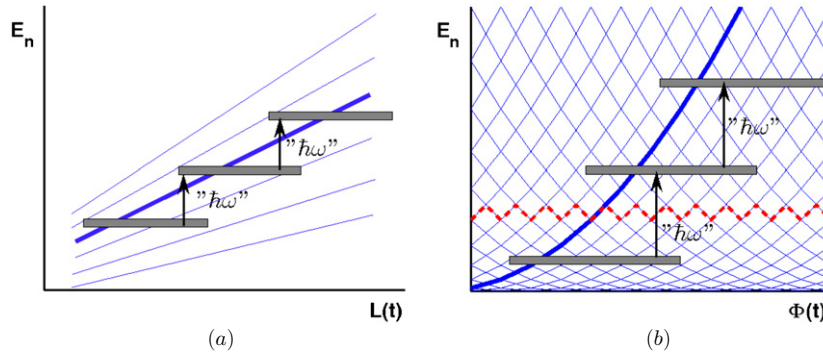


Figure 4. (a) Left panel: the energy levels of a one-dimensional box as a function of its width $L(t)$. For the purpose of comparison with other figures $L(t)$ is decreasing as we go to the right (the box becomes smaller) so the levels are going up. The solid line illustrates adiabatic dynamics, while the ‘jumps’ illustrate semiclassical dynamics. (b) Right panel: the energy levels of a one-dimensional ring as a function of the Aharonov–Bohm flux. The solid line illustrates diabatic dynamics, while the ‘jumps’ illustrate semiclassical dynamics. The dashed line illustrates adiabatic dynamics.

where Δ is the level spacing. In the case of the ‘moving wall’ problem this condition can be written as

$$V_{\text{wall}} \gg \frac{\hbar}{mL} \quad (7)$$

where L is the size of the box. It is easily verified that this condition is just the opposite of the adiabatic condition. The case of the EMF-driven ring is somewhat richer. The condition that defines the semiclassical regime becomes

$$V_{\text{EMF}} \gg \frac{\hbar v_E}{L} \quad (8)$$

where L is the length of the ring. It is easily verified that this condition is just the opposite of the diabaticity condition. The diabatic regime is defined as that where transitions between energy levels of a ‘free’ ring can be neglected. If there is a small scatterer inside the ring, a stronger condition than diabaticity is required in order to maintain adiabaticity:

$$V_{\text{EMF}} \ll (1 - g) \frac{\hbar v_E}{L} \quad (9)$$

where $g \sim 1$ is the transmission of the scatterer. The adiabatic regime is defined as that where transitions between the actual energy levels of the ring can be neglected. This is the regime where the Landau–Zener mechanism of transitions at avoided crossings [20, 21] becomes significant. The three regimes in the EMF-driven ring problem are illustrated in the diagram of figure 5.

Our main interest is in the non-trivial semiclassical regime as defined by equation (6). In order to reconcile our semiclassical intuition with the quantum Fermi Golden rule picture, we have to assume that the quantum dynamics self-generates a frequency $\hbar\omega = \delta E_{\text{cl}}$. Indeed, it has been argued in [7] that the non-perturbative mixing of levels on the small energy scales generate this frequency, while the re-normalized transitions on the large (coarse grained) energy scales are FGR like. However, an actual mathematical analysis of the dynamics has not been introduced and was left as an open problem. In section 7 we shall argue that these FGR-like energy jumps can be reinterpreted as unidirectional Bloch oscillations (figure 6).

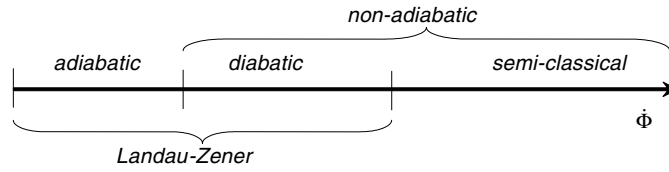


Figure 5. The three regimes in the EMF-driven ring problem. See the text.

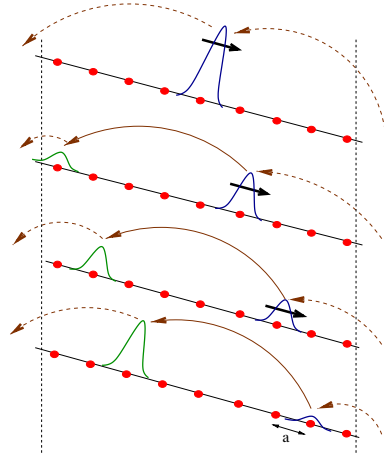


Figure 6. The unidirectional oscillations of Bloch electrons with $\propto 1/(n-m)$ hopping: as the wavepacket slides to the right it shrinks, while being re-injected on the left, where it re-emerges. This should be contrasted with conventional bi-directional oscillations of Bloch electrons with nearest neighbour hopping.

4. Particle pulsed by a step

The simplest example for a semiclassical energy jump is provided by the ‘step problem’. The time-dependent Hamiltonian is

$$\mathcal{H} = \frac{p^2}{2m} + \begin{cases} 0 & t < 0 \\ V_{\text{step}} & t \geq 0. \end{cases} \quad (10)$$

For this Hamiltonian ‘energy space’ is in fact ‘momentum space’, so it is more natural to refer to ‘momentum jumps’. Obviously, we can translate any small change in momentum to energy units via $\delta E = v_E \delta p$, where $v_E = (2E/m)^{1/2}$ is the velocity of the particle in the energy range of interest.

The phase space dynamics after kicking an initial momentum state p_0 at $t = 0$ is illustrated in figure 1(b). It is clear that the emerging momentum distribution is

$$\rho_t(p) = \left[1 - \frac{v_E t}{L} \right] \delta(p - p_0) + \frac{v_E t}{L} \delta(p - (p_0 + \delta p_{\text{cl}})) \quad (11)$$

where $\delta p_{\text{cl}} = -V_{\text{step}}/v_E$ and L is the spatial extent of the wavepacket. From here on we set $L = 1$ as implied by the standard density normalization of the momentum state $e^{ip_0 x}$. It is implicit in the following analysis that we assume a very extended wavepacket ($v_E t \ll L$).

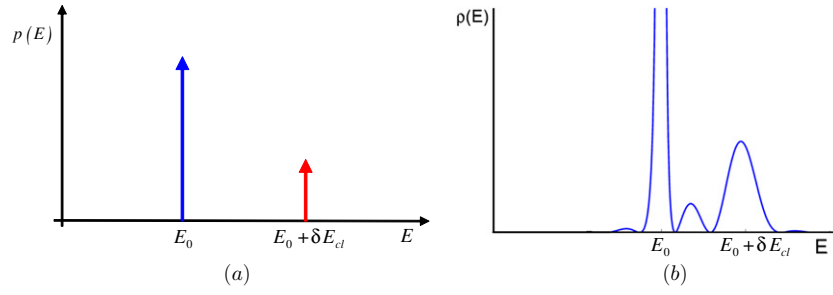


Figure 7. (a) Left panel: the classical energy distribution, equation (11), some time after a step potential is turned on. In this illustration $V_{\text{step}} > 0$. (b) Right panel: the corresponding quantum mechanical energy distribution calculated with equation (13).

The emerging momentum distribution can be characterized by its moments with respect to $p = p_0$. Namely,

$$\langle (p - p_0)^r \rangle = \delta p_{cl}^r \times v_E t \quad r = 1, 2, 3, 4, \dots \quad (12)$$

All the moments are finite and grow linearly with time. Below we are going to derive the quantum result. Omitting the trivial $\delta(p - p_0)$ term, and the back-reflection term, the final result for the forward scattering is

$$\rho_t(p) = |\langle p | \mathcal{U} | p_0 \rangle|^2 = \frac{\delta p_{cl}^2}{(p - p_0)^2} v_E^2 t^2 \sin^2 \left[\frac{1}{2} (p - (p_0 + \delta p_{cl})) v_E t \right] \quad (13)$$

for which

$$\langle (p - p_0)^r \rangle = \begin{cases} \delta p_{cl} \times v_E t - \sin(\delta p_{cl} v_E t) & \text{for } r = 1 \\ \delta p_{cl}^2 \times v_E t & \text{for } r = 2 \\ \infty & \text{for } r > 2. \end{cases} \quad (14)$$

Let us compare the energy distribution in the classical and quantum-mechanical cases (figure 7). As the time t becomes much larger than \hbar / V_{step} , the semiclassical peak is resolved. But we never get detailed QCC, because all the high ($r > 2$) moments of the distribution diverge.

It should be appreciated that the power law tails that we get here for the energy distribution are the ‘worst case’ that can be expected. They emerge because the phase space distribution is torn in the momentum direction. In space representation this reflects a discontinuity in the derivative of the wavefunction. This explains why the tails go like $1/p^4$. We are going to encounter the same type of power law tails also in the other examples.

4.1. Derivation of the quantum result

The rest of this section is devoted for the derivation of the quantum result and can be skipped in first reading. The momentum states are denoted as $|p\rangle$. In order to simplify the calculation we approximate the dispersion relation, within the energy window of interest, as linear $E = v_E k$. This implies that back-reflection is neglected. Once the step is turned on, $|p\rangle$ are no longer the stationary states. The new stationary states are

$$|k\rangle \mapsto \Theta(-x) e^{ikx} + \Theta(x) e^{i(k+u)x} \quad (15)$$

where we use the notation $u = \delta p_{cl}$. Note that these form a complete orthonormal set in the sense $\langle k_1 | k_2 \rangle = 2\pi \delta(k_1 - k_2)$. The transformation matrix from the old to the new basis is

$$\langle p | k \rangle = \int_{-\infty}^0 e^{-i(p-k)x} dx + \int_0^{\infty} e^{-i(p-k-u)x} dx \quad (16)$$

$$= \pi \delta(p - k) + \frac{i}{p - k} + \pi \delta(p - k - u) - \frac{i}{p - k - u}. \quad (17)$$

Before we go on with the calculation we note that the following elementary integral can be found in any mathematical handbook:

$$\int_{-\infty}^{\infty} \frac{dk}{2\pi} \frac{1}{(k - p_2)(k - p_1)} e^{ikt} = \frac{i}{2(p_2 - p_1)} (e^{ip_2 t} - e^{ip_1 t}) \quad p_2 \neq p_1, \quad t > 0.$$

We note that the result on the RHS is finite for $p_2 = p_1$ while in fact it should diverge. This suggests that there is a missing delta term $C e^{ip_2 t} \delta(p_2 - p_1)$ where C is a constant. In order to find this constant we have regularized this Fourier integral:

$$\begin{aligned} \lim_{\delta \rightarrow 0} \int_{-\infty}^{\infty} \frac{dk}{2\pi} \frac{k - p_2}{(k - p_2)^2 + \delta^2} \frac{k - p_1}{(k - p_1)^2 + \delta^2} e^{ikt} \\ = \frac{i}{2(p_2 - p_1)} (e^{ip_2 t} - e^{ip_1 t}) + \frac{\pi}{2} e^{ip_2 t} \delta(p_2 - p_1) \quad t > 0. \end{aligned}$$

With the above we can calculate the matrix elements of the evolution operator:

$$\begin{aligned} \langle p | \mathcal{U} | p_0 \rangle &= \sum_k e^{-iE_k t} \langle p | k \rangle \langle k | p_0 \rangle = \frac{1}{2\pi} \int_{-\infty}^{\infty} e^{-iv_E k t} \langle p | k \rangle \langle k | p_0 \rangle dk \\ &= \pi \delta(p - p_0) (e^{iv_E p t} + e^{iv_E (p+u)t}) + \frac{i u}{(p - p_0)(p - p_0 - u)} (e^{iv_E (p_0+u)t} - e^{iv_E p t}). \end{aligned} \quad (18)$$

We have $\langle p | \mathcal{U}(t=0) | p_0 \rangle = 2\pi \delta(p - p_0)$ as required. The interesting part of this expression is the second terms which is non-vanishing for $p \neq p_0$. Taking its absolute value and squaring we get after some algebra equation (13).

5. Particle in a box with a moving wall

5.1. The Schrödinger equation

We consider a particle in an infinite well. The left wall is assumed to be fixed at $x = x_0$, while the right wall at $x = X(t)$ is moving with constant velocity $\dot{X} = V_{\text{wall}}$. The size of the box is $L(t) = X(t) - x_0$. Classically, the dynamics is very simple: each time that the particle hits the moving wall its energy jumps by $\delta E_{cl} = 2mvV_{\text{wall}}$. In the quantum mechanical case, we work in the adiabatic basis. The adiabatic energy levels and the eigenstates for a given value of L are

$$E_n = \frac{1}{2m} \left(\frac{\pi \hbar}{L} n \right)^2 \quad (19)$$

$$\Psi^{(n)}(x) = (-1)^n \sqrt{\frac{2}{L}} \sin\left(\frac{\pi n}{L} x\right) \quad (20)$$

We use the standard prescription in order to write the Schrödinger equation in the adiabatic basis. Using the notations of [22], the equation is written as

$$\frac{da_n}{dt} = -\frac{i}{\hbar} E_n a_n + i\dot{X} \sum_m A_{nm} a_m \quad (21)$$

where

$$A_{nm} = i \left\langle \Psi^{(n)} \left| \frac{\partial}{\partial X} \Psi^{(m)} \right. \right\rangle. \quad (22)$$

Hence, the Schrödinger equation for the problem in the adiabatic basis is [3, 6]

$$\frac{da_n}{dt} = -\frac{i}{\hbar} E_n a_n - \frac{V_{\text{wall}}}{L} \sum_{m(\neq n)} \frac{2nm}{n^2 - m^2} a_m \quad (23)$$

5.2. The generated dynamics

Let us assume that the initial preparation is $a_n(0) = \delta_{nm}$. The mean level spacing for the 1D box is $\Delta = \pi \hbar v_E / L$. If $\delta E_{\text{cl}} \ll \Delta$ one finds out, by inspection of equation (23), that the dynamics is adiabatic, meaning that $a_n(t) \sim \delta_{nm}$. On the other hand, if $\delta E_{\text{cl}} \gg \Delta$, one expects to find a semiclassical transition $E \mapsto E + \delta E_{\text{cl}}$.

How can we explain the $E \mapsto E + \delta E_{\text{cl}}$ transition from quantum-mechanical point of view? For this purpose we can adopt the core-tail picture of [23]: the ‘core’ consists of the levels that are mixed non-perturbatively; the ‘tail’ is formed by first-order transitions from the core. Originally this picture has been applied to analyse the energy spreading in ‘quantum chaos’ driven systems. Here, the (non-chaotic) moving wall problem allows a much simpler application [7]. The analysis is carried out in two steps which are summarized below.

The first step in the ‘core-tail’ picture is to analyse the *parametric evolution* which is associated with equation (23). This means to solve equation (23) without the first term on the RHS. (This is the so-called sudden limit). Obviously, the resultant $\tilde{a}_n(t)$ is a function of $\delta X = V_{\text{wall}} t$, while V_{wall} by itself makes no difference. The solution depends only on the endpoints $x(0)$ and $x(t)$. By careful inspection of equation (23), one observes that a level is mixed with the nearby level whenever the wall is displaced a distance $\lambda_E/2$, where $\lambda_E = 2\pi \hbar / (m v_E)$ is the de Broglie wavelength. The time scale which is associated with this effect is obviously

$$\tau_{\text{qm}} = \frac{\lambda_E/2}{V_{\text{wall}}}. \quad (24)$$

The second step is to analyse the actual time evolution. This means to take into account the effect of the first term on the RHS of equation (23) and to understand how the resultant $a_n(t)$ differs from $\tilde{a}_n(t)$. One observes that the ‘parametric’ mixing of nearby levels modulates the transition amplitude. The modulation frequency is

$$‘\omega’ = \frac{2\pi}{\tau_{\text{qm}}}. \quad (25)$$

Once combined with the FGR equation (25) it leads to the anticipated semiclassical result equation (5). It is not difficult to argue that the period of this semiclassical transition is

$$\tau_{\text{cl}} = \frac{2L}{v_E} \quad (26)$$

which is the time to make one round between the walls of the well. Since we are dealing with a simple 1D system this coincides with the Heisenberg time:

$$t_{\text{H}} = \frac{2\pi \hbar}{\Delta} = \tau_{\text{cl}}. \quad (27)$$

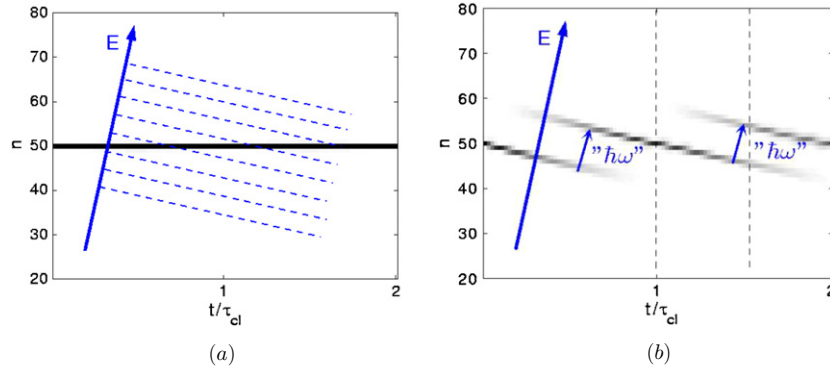


Figure 8. Density plots of the probability distribution as a function of time for the moving wall problem. (a) Left panel: adiabatic regime. The probability stays at the same level. In order to clarify the connection with figure 4(a) we have added an E axis. The constant energy dashed lines are for guiding the eye. The populated adiabatic level goes up in energy which implies that the particle is steadily increasing its energy. (b) Right panel: semiclassical regime. The probability jumps in energy space. Note that with respect to the E axis we have the steps of figure 4(a). The parameters of these simulations were $L = m = \hbar = 1$ and $V_{\text{wall}} = 0.1\pi$ for (a) and $V_{\text{wall}} = 5\pi$ for (b). Note that for $n = 50$ the classical period is $\tau_{\text{cl}} = 0.0127$. The vertical dashed lines indicate two representative times $t = \tau_{\text{cl}}$ and $t = 1.5\tau_{\text{cl}}$.

The ratio $\tau_{\text{cl}}/\tau_{\text{qm}}$ determines the number of nearby level transitions per period. Obviously, the semiclassical condition equation (7) requires this ratio to be much larger than unity. The disadvantage of the above heuristic picture is that it does not lead to a satisfactory quantitative results. Therefore, in later sections we discuss an optional route of analysis via a reduction to a tight binding model.

5.3. Numerical simulation

The solution of equation (23) becomes very simple if we make the approximation $L(t) \approx L_0$. This holds as long as the wall displacement is small. We have verified that the associated numerical error is very small. Using units such that $L_0 = m = \hbar = 1$ we define a diagonal matrix $\mathbf{E} = \text{diag}\{\pi^2 n^2/2\}$ and a non-diagonal matrix, $\mathbf{W} = \{-i2\alpha nm/(n^2 - m^2)\}$ with zeros along the diagonal, and where $\alpha = V_{\text{wall}}/L$. The evolution matrix in the adiabatic basis is obtained by exponentiation:

$$\mathbf{U}(t) = \exp[-it(\mathbf{E} + \mathbf{W})]. \quad (28)$$

Figure 8 illustrates the time dependence of probability distribution $|a_n(t)|^2$ for a particle initially prepared at $n_0 = 50$. Figure 8(a) displays the solution in the adiabatic regime: the particle stays at the same level. Figure 8(b) displays the solution in the semiclassical regime: at each moment the particle partially stays at the same energy and partially makes classical-like transition to the next energy strip. Figure 9 highlights the energy splitting of the wavepacket during the transition.

If we want to avoid the $L(t) \approx L_0$ approximation, the price is a time-dependent \mathbf{E} and \mathbf{W} matrices. Then the calculation should be done in small dt time steps:

$$\mathbf{U}(t) = \prod_{t'=dt}^t \exp[-i dt \mathbf{W}(t')] \exp[-i dt \mathbf{E}(t')]. \quad (29)$$

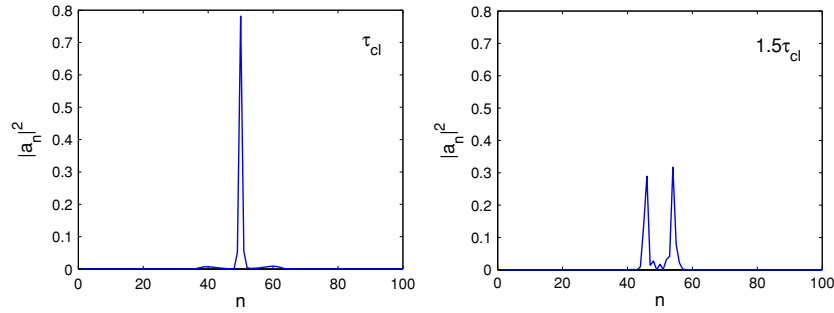


Figure 9. Plots of the probability distribution $|a_n|^2$ at the two representative times that were indicated by the vertical dashed lines in the previous figure. In the classical limit, the energy distribution consists of delta peaks instead of broadened peaks, in complete analogy with figure 7.

The state of the system is described by a truncated column vector $\mathbf{a} = \{a_n\}$ of length N . Optionally, it is possible to represent the state of the system in the Fourier-transformed basis. The elements A_k of the Fourier-transformed vector are labelled by $k = (2\pi/N)\tilde{n}$, where $\tilde{n} \bmod(N)$ is an integer. The practical implementation of equation (29) is greatly simplified if \mathbf{W}_{nm} is a function of the difference $n - m$. In such a case \mathbf{W} is transformed into a diagonal matrix $\tilde{\mathbf{W}}$. Consequently, one can use the standard fast Fourier transform (FFT) algorithm in order to propagate a given state vector. Namely,

$$\mathbf{a}(t) = \prod_{t'=dt}^t \text{FFT}^{-1} \exp[-idt \tilde{\mathbf{W}}(t')] \text{FFT} \exp[-idt \mathbf{E}(t')] \mathbf{a}(0) \quad (30)$$

where both \mathbf{E} and $\tilde{\mathbf{W}}$ are diagonal. In the moving wall problem \mathbf{W}_{nm} is mainly proportional to $1/(n - m)$, so the FFT method is applicable if we restrict the energy range of interest. In the next section, we shall consider the EMF-driven ring problem, leading to a very similar evolution equation, where the FFT method is strictly applicable.

6. Particle in an EMF-driven ring

6.1. The Schrödinger equation

We consider a 1D ring driven by an EMF (figure 3). The EMF is induced by a time-dependent flux which is described by the vector potential

$$A(x, t) = \Phi(t)\delta(x - x_0). \quad (31)$$

This means that the electric field is

$$\mathcal{E}(x) = V_{\text{EMF}}\delta(x - x_0) \quad (32)$$

where $V_{\text{EMF}} = -\dot{\Phi} = \text{const}$. The Hamiltonian that generates the dynamics is

$$\mathcal{H}(\Phi(t)) = \frac{1}{2m} \left(\hat{p} - \frac{e}{c} A(\hat{x}, t) \right)^2 \quad (33)$$

with periodic boundary conditions over x . The length of the ring is L .

Classically, the dynamics is very simple: each time that the particle crosses $x = x_0$ its energy jumps by $\delta E_{\text{cl}} = eV_{\text{EMF}}$. In the quantum mechanical case, it is convenient to work in

the so-called diabatic basis. The diabatic energy levels for a given value of Φ are

$$E_n = \frac{1}{2m} \left(\frac{2\pi\hbar}{L} \right)^2 \left(n - \frac{\Phi}{\Phi_0} \right)^2 \quad (34)$$

where $\Phi_0 = 2\pi\hbar c/e$, see figure 4. The Schrödinger equation that describes the time evolution in the diabatic basis is found using the same procedure as in the case of the moving wall. We have to find A_{nm} as defined in equation (22) where now $X = \Phi$. The only extra difficulty is in finding the eigenstates $\Psi^{(n)}$ of equation (33) because $A(x)$ depends on x . The calculation becomes much simpler if we realize that they are related by a gauge transformation to the eigenstates $\tilde{\Psi}^{(n)}$ of a much simpler Hamiltonian:

$$\tilde{\mathcal{H}} = \frac{1}{2m} \left(p - \frac{e\Phi}{cL} \right)^2. \quad (35)$$

Namely,

$$\Psi^{(n)}(x) = \exp\left(\frac{ie}{\hbar c} \Lambda(x)\right) \tilde{\Psi}^{(n)}(x) \quad (36)$$

$$= \exp\left(\frac{ie}{\hbar c} \Lambda(x)\right) \times \frac{1}{\sqrt{L}} \exp\left(i \frac{2\pi n}{L} x\right) \quad (37)$$

$$= \frac{1}{\sqrt{L}} \exp\left(i \frac{2\pi}{L} \left(\frac{\Phi}{\Phi_0} + n \right) x\right) \quad (38)$$

where in the last line we set $x_0 = 0$ and the gauge function is

$$\Lambda(x) = \frac{\Phi}{L} x. \quad (39)$$

Using the above result we get

$$A_{nm} = -\frac{i}{\Phi_0} \frac{1}{n-m} \quad (40)$$

and accordingly

$$\frac{da_n}{dt} = -\frac{i}{\hbar} E_n a_n + \frac{V_{\text{EMF}}}{\Phi_0} \sum_{m(\neq n)} \frac{1}{n-m} a_m. \quad (41)$$

6.2. The generated dynamics

The dynamics of an EMF-driven ring is very similar to the dynamics in the moving wall problem. This is obvious from the phase space picture and also by the inspection of the equation for $a_n(t)$. Also the ‘core-tail’ heuristic picture of section 5.2 is easily adapted. The parametric scale that signifies mixing of nearby levels is now $\delta X = \Phi_0$ instead $\delta X = \lambda_E/2$ leading to the quantum time scale

$$\tau_{\text{qm}} = \frac{\Phi_0}{V_{\text{EMF}}}. \quad (42)$$

The classical period is

$$\tau_{\text{cl}} = \frac{L}{v_E} \quad (43)$$

and the semiclassical condition can be written as $\tau_{\text{qm}} \ll \tau_{\text{cl}}$.

Since the energies are time dependent we have to use equation (29) for the calculation of the time evolutions. Furthermore, \mathbf{W} is diagonal in the momentum representation,

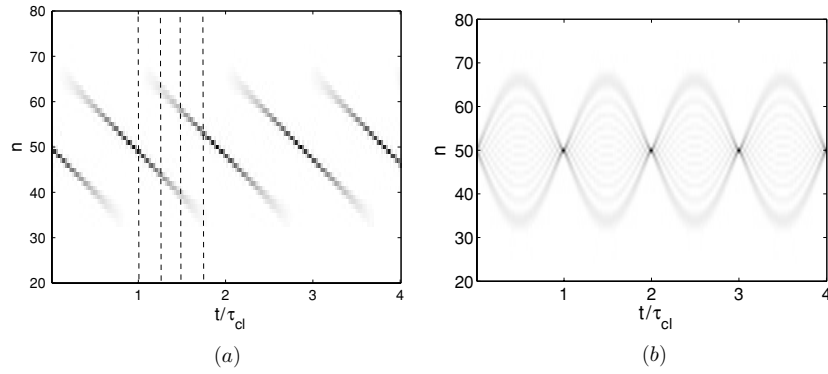


Figure 10. (a) Density plots of the probability distribution as a function of time for the EMF-driven ring problem. See the caption of figure 8 for presentation details. The parameters are $L = m = \hbar = e = 1$ with $V_{\text{EMF}} = 588\,840$. Note that for $n = 50$ the classical period is $\tau_{\text{cl}} = 0.000\,21$. This is approximately the same as solving the wavepacket dynamics for Bloch electron in electric field, equation (44), with $\alpha = 93\,717$ and $\varepsilon = 31\,416$. (b) Wavepacket dynamics for Bloch electron in electric field with near-neighbour hopping. The parameters are $m = \hbar = e = 1$ with $\alpha = 14\,139$ and $\varepsilon = 3141.6$.

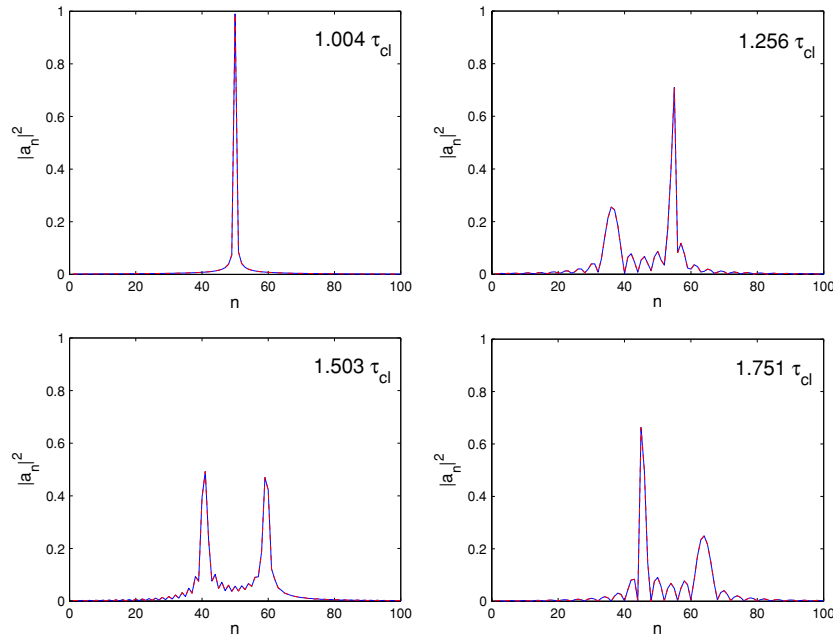


Figure 11. Plots of the probability distribution $|a_n|^2$ at representative times (as indicated). The solid lines are the solution of equation (44) for Bloch electrons, while the dotted lines are the exact numerical solutions for the EMF-driven ring, taking into account the quadratic (rather than linear) dependence of the eigenenergies on Φ .

and therefore we can use the FFT method, equation (30), with $\tilde{W} = \text{diag}\{-\alpha(k - \pi)\}$, where $k = (2\pi/N)\tilde{n}$ is defined mod(2π). The results of the simulations are presented in figures 10(a) and 11. We shall further discuss these results in the next sections.

7. Bloch electrons in a constant electric field (I)

If we focus our interest in small energy interval, then in both cases (moving wall, driven ring) the Schrödinger equation in the adiabatic basis is approximately the same as that of an electron in a tight binding model, where n is re-interpreted as the site index:

$$\frac{da_n}{dt} = -iE_n a_n + \alpha \sum_{m(\neq n)} \frac{1}{n-m} a_m \quad (44)$$

with $E_n = \varepsilon n$. We use from here on $\hbar = 1$ units. The scaled rate of the driving α is re-interpreted as the hopping amplitude between sites, while the levels spacing ε is re-interpreted as an electric field. Assuming that the electron is initially at the site n_0 , we would like to find out what is the probability distribution

$$\rho_t(n) = |a_n(t)|^2. \quad (45)$$

It is obvious that the adiabatic regime $\alpha \ll \varepsilon$ corresponds to a large electric field that localizes the electron at its original site. In the other extreme ($\alpha \gg \varepsilon$), if the effect of ε could have been ignored, we would observe unbounded Bloch ballistic motion. The effect of finite ε is to turn this motion into Bloch oscillations. We shall find below that the electron performs periodic motion which we illustrate in figure 6: while the wavepacket drifts with the electric field to the right, it shrinks and disappears, and at the same time re-emerges on the left. If we run the simulation as a movie, it looks as if the motion is from left to right. Still it is bounded in space due to this ‘re-injection’ mechanism.

First of all we solve the equation for $\varepsilon = 0$. The Hamiltonian is diagonal in the momentum basis k and therefore the general solution is

$$a_n(t) = \sum_k A_k e^{i(kn - \omega_k t)} = \int_0^{2\pi} \frac{dk}{2\pi} A_k e^{i(kn - \omega_k t)}. \quad (46)$$

The dispersion relation is found by transforming the Hamiltonian to the k basis:

$$\omega_k = i\alpha \sum_{n(\neq m)} \frac{e^{-ik(n-m)}}{n-m} = \alpha[\pi - k]. \quad (47)$$

If we place at $t = 0$ an electron at site n_0 , then $a_n = \delta_{n,n_0}$, and hence $A_k = e^{-ikn_0}$. Then, we get

$$a_n(t) = \frac{\sin \pi \alpha t}{\pi(\alpha t + n - n_0)}. \quad (48)$$

Turning to the general case with $\varepsilon \neq 0$ we substitute $a_n(t) = c_n(t) e^{-iE_n t}$ and get the equation

$$\frac{dc_n}{dt} = \alpha \sum_{m(\neq n)} \frac{e^{i(n-m)\varepsilon t}}{n-m} c_m. \quad (49)$$

This more complicated equation is still diagonal in the k basis:

$$\frac{dC_k}{dt} = -i\omega_k(t) C_k \quad (50)$$

where

$$\omega_k(t) = \alpha[\pi - \text{mod}(k + \varepsilon t, 2\pi)] \quad (51)$$

and its solutions is

$$C_k(t) = C_k(t=0) \exp \left[-i \int_0^t \omega_k(t') dt' \right]$$

$$= \begin{cases} \exp \left(-ikn_0 + i\alpha \left((k - \pi)t + \frac{\varepsilon t^2}{2} \right) \right) & \text{for } \varepsilon > 0 \text{ and } 0 < k < \bar{k} \\ \exp \left(-ikn_0 + i\alpha \left((k - 3\pi)t + \frac{\varepsilon t^2}{2} + \frac{2\pi(2\pi - k)}{\varepsilon} \right) \right) & \text{for } \varepsilon > 0 \text{ and } \bar{k} < k < 2\pi \\ \exp \left(-ikn_0 + i\alpha \left((k - \pi)t + \frac{\varepsilon t^2}{2} + \frac{2\pi k}{\varepsilon} \right) \right) & \text{for } \varepsilon < 0 \text{ and } 0 < k < \bar{k} \\ \exp \left(-ikn_0 + i\alpha \left((k + \pi)t + \frac{\varepsilon t^2}{2} \right) \right) & \text{for } \varepsilon < 0 \text{ and } \bar{k} < k < 2\pi \end{cases}$$

which is valid for $0 < t < 2\pi/|\varepsilon|$ and should be continued periodically in time. We have used the notation $\bar{k} = -\varepsilon t \bmod(2\pi)$. Now we can go back to position representation:

$$c_n(t) = \int_0^{\bar{k}(t)} \frac{dk}{2\pi} C_k e^{ikn} + \int_{\bar{k}(t)}^{2\pi} \frac{dk}{2\pi} C_k e^{ikn}. \quad (52)$$

Taking the absolute value and squaring we get the following result for the probability distributions:

$$\rho_t(n) = \left(2 \frac{\alpha}{\varepsilon} \right)^2 \frac{\sin^2 \left(\frac{1}{2} \varepsilon t \left(n - n_0 + \alpha \left(t - \frac{2\pi}{|\varepsilon|} \right) \right) \right)}{\left(n - n_0 + \alpha t \right)^2 \left(n - n_0 + \alpha \left(t - \frac{2\pi}{|\varepsilon|} \right) \right)^2}. \quad (53)$$

The above formula is valid for $0 < t < 2\pi/|\varepsilon|$ and it should be continued periodically in time. Figures 6 and 10(a) illustrate the dynamics both schematically and numerically. In the next section we further discuss the nature of this dynamics.

8. Bloch electrons in a constant electric field (II)

In order to appreciate the significance of the $\propto 1/(n - m)$ hopping we again solve the problem of Bloch electrons in a constant electric field, but this time with the ‘conventional’ nearest neighbour hopping:

$$\frac{da_n}{dt} = -iE_n a_n + \frac{\alpha}{2} [a_{n+1} - a_{n-1}] \quad (54)$$

with $E_n = \varepsilon n$. The initial preparation at $t = 0$ is $a_n = \delta_{n,n_0}$. We substitute $a_n = e^{-iE_n t} c_n$ and get

$$\frac{dc_n}{dt} = \frac{\alpha}{2} (e^{-i\varepsilon t} c_{n+1} - e^{i\varepsilon t} c_{n-1}). \quad (55)$$

This equation becomes diagonal in the k basis:

$$\frac{dC_k}{dt} = -i\omega_k(t) C_k \quad (56)$$

where

$$\omega_k(t) = \alpha \sin(\varepsilon t + k). \quad (57)$$

Its solutions is

$$C_k(t) = C_k(t=0) \times \exp \left[-i \int_0^t \omega_k(t') dt' \right]. \quad (58)$$

Solving the above integral and making the inverse Fourier transform we obtain

$$c_n(t) = J_{n-n_0} \left(\frac{2\alpha}{\varepsilon} \sin \left(\frac{1}{2} \varepsilon t \right) \right) \quad (59)$$

where $J(\cdot)$ is the Bessel function of the first kind. Taking the absolute value and squaring we get the probability distribution:

$$\rho_t(n) = \left| J_{n-n_0} \left(\frac{2\alpha}{\varepsilon} \sin \left(\frac{1}{2} \varepsilon t \right) \right) \right|^2. \quad (60)$$

Figure 10(b) illustrates the dynamics. As in the previous problems we can distinguish between two time scales. One is related to the diagonal part of the Hamiltonian, and the other one to the hopping term. Keeping the same notation as in previous sections these are

$$\tau_{\text{cl}} = 2\pi/\varepsilon \quad (61)$$

$$\tau_{\text{qm}} = 1/\alpha. \quad (62)$$

The nature of the dynamics in the case of $\propto 1/(n-m)$ hopping and in the case of near-neighbour hopping is quite different, as it can be appreciated by comparing figures 10(a) and (b). This is related to the additional symmetries in the latter case. In order to explain this point let us use the notation $U(\alpha, \varepsilon)$ that emphasizes that the evolution depends on two parameters, the first one is associated with the kinetic term $\mathbf{W} = w(\hat{p})$ and the other one with the potential term $\mathbf{E} = \varepsilon(\hat{x})$. For clarity we use \hat{x} for the position coordinate and \hat{p} for the quasi-momentum. In both cases, we have the anti-unitary symmetry $(x, p) \mapsto (x, -p)$ that maps \mathbf{E} to \mathbf{E} and \mathbf{W} to $-\mathbf{W}$. Consequently, $U(\alpha; \varepsilon)$ is mapped to $U(\alpha; -\varepsilon)$. This implies that the spreading does not depend on the direction of the electric field. This is a peculiarity of tight binding models. The conventional time reversal symmetry, for which the kinetic term \mathbf{W} is left invariant, is $(x, p) \mapsto (x, \pi - p)$. This symmetry characterizes the near-neighbour hopping, but not the $\propto 1/(n-m)$ hopping. This symmetry implies that the spreading looks the same if we reverse the signs of both α and ε , which is like reversing the time. If we combine the two symmetries we deduce that the dynamics, in the case of the near-neighbour hopping, should be indifferent to the sign of α . Note that the combined symmetry that leads to this conclusion is the unitary mapping $(x, p) \mapsto (x, p + \pi)$. Thus, in both cases ($\propto 1/(n-m)$ hopping and near-neighbour hopping) we have generalized Bloch oscillations, but in the former case they are unidirectional (figure 6), while in the latter case they are bi-directional.

9. Discussion

Within Linear response theory (LRT) the energy absorption of a quantum system is determined by the correlation function of the perturbation term. In general, one can argue that there is a very good QCC for the correlation functions, and hence one expects *restricted* QCC in the energy absorption process. The persistence of *restricted* QCC in the $t \rightarrow \infty$ limit requires the additional assumption of having a coarse-grained Markovian-like behaviour for long times. Depending on the context one should further assume that the environment supplies both weak decoherence effect that makes the break time t^* irrelevant and a weak relaxation effect so as to achieve a steady state. Then it is possible to use the same argumentation as in the derivation of the central limit theorem in order to argue that all the higher moments become Gaussian like.

Thus, the common perception is that the leading result for the response of a driven system should be the same classically and quantum mechanically. For example, such is the case if one

calculates the conductance of a diffusive ring [24]: the leading order result is just the Drude expressions, and on top there are weak localization corrections.

The above reasoning illuminates that the long time response is based on the short time analysis. Moreover, one realizes that the second moment of the evolving energy distribution has a special significance. Still, all the above observations are within a very restrictive framework of assumptions. In practice, it is of much interest to explore the limitations of LRT and to obtain a more general theory for response.

The theory for the response of closed isolated driven quantized chaotic mesoscopic systems is far from being trivial, even if the interactions between the particles are neglected. In the case of a generic quantized chaotic systems two energy scales are involved: the mean level spacing $\Delta \propto \hbar^d$, where $d = 2, 3$ is the dimensionality of the system, and the semiclassical energy scale \hbar/τ_{cl} . It is implied (see the mini-review of [25]) that there are generically three regimes depending on the rate \dot{X} of the driving:

- The adiabatic (Landau–Zener) regime.
- The Fermi-golden-rule (FGR, Kubo) regime.
- The semiclassical (non-perturbative) regime.

Most of the literature in mesoscopic physics is dedicated to the study of the dynamics in either the adiabatic or the FGR regimes. The existence of a non-perturbative regime [25, 26] is not yet fully acknowledged, though it has been established numerically in the RMT context [27].

Driven one-dimensional systems are non-generic because typically the semiclassical energy scale coincides with the mean level spacing. In other words, the Heisenberg time $t_H = 2\pi\hbar/\Delta$ is the same as the classical time τ_{cl} rather than being much larger. Indeed, we have seen that in the ‘moving wall’ problem we have just two regimes: the adiabatic regime and the semiclassical regime.

The EMF-driven ring is a prototype problem in mesoscopic physics. It is richer than the ‘moving wall’ problem because a small scatterer introduces a very small energy scale, the level splitting, and hence we have three regimes rather than two: adiabatic, diabatic and semiclassical.

The semiclassical regime in the study of EMF-driven rings has not been explored so far. One important observation is that contrary to LRT the gauge of the vector potential *does matter*. Most of past studies assume that the vector potential is $A(x, t) = \Phi(t)/L$. It is true that in LRT the same result for the conductance is obtained with $\tilde{A}(x, t) = \Phi(t)\delta(x - x_0)$. If we try to go from $\tilde{A}(x, t)$ to $A(x, t)$ using a gauge transformation, the ‘price’ is a modified $V(x)$ that features a linear ramp with a step-like drop at $x = x_0$. This modification of $V(x)$ can be neglected only in the LRT regime. The semiclassical condition of equation (6) is just that opposite of this LRT requirement.

The semiclassical dynamics implies diffractive energy spreading. The mixing of levels in the small energy scales induces jumps in energy space. The realization that this diffractive energy spreading can be re-interpreted using a tight binding Bloch model follows in spirit the celebrated reduction [1] of dynamical localization in periodically kicked systems to a tight binding Anderson problem. An interesting feature is the hopping that goes like $\propto 1/(n - m)$. This hopping leads to a unidirectional rather than bi-directional Bloch oscillations, as implied by the semiclassical reasoning.

Acknowledgments

We thank Tsachy Holovinger for preparing the first version of the ‘moving wall’ simulation. AS thanks V Golland for fruitful discussions that helped solving the ‘Bloch electrons’ problem.

The research was supported by the Israel Science Foundation (grant no 11/02) and by a grant from the DIP, the Deutsch–Israelische Projektkooperation.

Appendix. The robustness of restricted QCC

The simplest way to illuminate the robustness of the second moment is by adopting a heuristic phase space picture language. Given two operators $\hat{A} = A(\hat{x}, \hat{p})$ and $\hat{B} = B(\hat{x}, \hat{p})$, with Wigner–Weyl representation $A_{\text{WW}}(x, p)$ and $B_{\text{WW}}(x, p)$ we have the exact identity

$$\text{trace}(\hat{A}\hat{B}) = \int \frac{dx dp}{2\pi} A_{\text{WW}}(x, p) B_{\text{WW}}(x, p). \quad (\text{A.1})$$

If we can justify the replacement of $A_{\text{WW}}(x, p)$ by $A(x, p)$ and $B_{\text{WW}}(x, p)$ by $B(x, p)$ then we get QCC. The rule of the thumb is that in order to justify such an approximation the phase space contours of $A(x, p)$ and $B(x, p)$ should be significantly different. Otherwise the transverse structure of the Wigner–Weyl functions should be taken into account. This reasoning can be regarded as a phase space version of the stationary phase approximation.

Let $\hat{A} = [H(\hat{x}, \hat{p})]^r$ be the r th power of the Hamiltonian $\mathcal{H} = H(\hat{x}, \hat{p})$ and let be $\hat{B} = \rho(H_0(\hat{x}, \hat{p}))$ a stationary preparation with the Hamiltonian $\mathcal{H}_0 = H_0(\hat{x}, \hat{p})$. In such a case $\text{trace}(\hat{A}\hat{B})$ is the r th moment $\langle \mathcal{H}^r \rangle$ of the energy. If $H = H_0 + \lambda V$, and λ is not large enough, then we do not have detailed QCC. This is discussed thoroughly in [28]. But at the same time, irrespective of λ , restricted QCC is robust. The reason is that for the first two moments we have the identities

$$\langle \mathcal{H} \rangle = \langle \mathcal{H}_0 \rangle + \langle \hat{V} \rangle \quad (\text{A.2})$$

$$\langle \mathcal{H}^2 \rangle = \langle \mathcal{H}_0^2 \rangle + 2\langle \mathcal{H}_0 \rangle \langle \hat{V} \rangle + \langle \hat{V}^2 \rangle. \quad (\text{A.3})$$

Thus the calculation of $\text{trace}(\hat{A}\hat{B})$ with $\hat{A} = [H(\hat{x}, \hat{p})]^r$ reduces to the calculation of $\text{trace}(\hat{A}\hat{B})$ with $\hat{A} = [V(\hat{x}, \hat{p})]^r$. We assume that V and H are not related in any special way. It follows that we have robust QCC for all the moments of V , and consequently also for the first two moments of H , irrespective of λ .

In order to generalize the above reasoning to time-dependent Hamiltonians, it is convenient to adopt the Heisenberg picture. Given that the system is prepared in a stationary state at $t = 0$, one can prove that

$$\langle \mathcal{H}(t)^2 \rangle_0 - \langle \mathcal{H}(0)^2 \rangle_0 = \langle (\mathcal{H}(t) - \mathcal{H}(0))^2 \rangle_0 \quad (\text{A.4})$$

where $\mathcal{H}(t)$ is the Hamiltonian $\mathcal{H}(X(t))$ in the *Heisenberg picture*. Such relation cannot be generalized to higher moments because of lack of commutativity. Using

$$\frac{d\mathcal{H}}{dt} = \frac{\partial \mathcal{H}}{\partial t} = \dot{X} \hat{V}(t) \quad (\text{A.5})$$

where $V \equiv \partial \mathcal{H} / \partial X$, we can express $\langle (\mathcal{H}(t) - \mathcal{H}(0))^r \rangle_0$ as an integral over the correlation functions of the perturbation $V(t)$. The QCC for these correlation functions is robust, and hence the QCC for the second moment is also robust.

References

- [1] Fishman S, Gempel D R and Prange R E 1982 *Phys. Rev. Lett.* **49** 509
Gempel D R, Prange R E and Fishman S 1984 *Phys. Rev. A* **29** 1639
- [2] Cohen D and Kottos T 2003 *J. Phys. A: Math. Gen.* **36** 10151
- [3] Doescher S W and Rice M H 1969 *Am. J. Phys.* **37** 1246

- [4] Makovski A J and Demebinski S T 1986 *Phys. Rev. Lett.* **56** 290
- [5] Jos J V and Cordery R 1986 *Phys. Rev. Lett.* **56** 290293
- [6] Cohen D, Barnett A and Heller E J 2001 *Phys. Rev. E* **63** 46207
- [7] Cohen D 2002 *Phys. Rev. E* **65** 026218 (section VIII)
- [8] Wannier G H 1960 *Phys. Rev.* **117** 432
- [9] Zak J 1968 *Phys. Rev. Lett.* **20** 1477
- [10] Zak J 1968 *Phys. Rev.* **168** 686
- [11] Rabinovitch A and Zak J 1972 *Phys. Lett. A* **40** 189
- [12] Rabinovitch A 1977 *Phys. Lett. A* **59** 475
- [13] Emin D and Hart C F 1987 *Phys. Rev. B* **36** 7353
- [14] Hart C F 1988 *Phys. Rev. B* **38** 2158
- [15] Hart C F and Emin D 1988 *Phys. Rev. B* **37** 6100
- [16] Mendez E E, Agullo-Rueda F and Hong J M 1988 *Phys. Rev. Lett.* **60** 2426
- [17] Zak J 1991 *Phys. Rev. B* **43** 4519
- [18] Leo J and MacKinnon A 1991 *Phys. Rev. B* **43** 5166
- [19] Zak J 1996 *J. Phys.: Condens. Matter* **8** 8265
- [20] Gefen Y and Thouless D J 1987 *Phys. Rev. Lett.* **59** 1752
- [21] Wilkinson M 1988 *J. Phys. A: Math. Gen.* **21** 4021
- [22] Cohen D 2003 *Phys. Rev. B* **68** 155303
- [23] Cohen D 2000 *Ann. Phys., NY* **283** 175
- [24] Kamenev A and Gefen Y 1995 *Int. J. Mod. Phys. B* **9** 751
- [25] Cohen D 2002 *Dynamics of Dissipation: Proc. 38th Karpacz Winter School of Theoretical Physics* ed P Garbaczewski and R Olkiewicz (Berlin: Springer) (Preprint [quant-ph/0403061](#))
- [26] Cohen D 1999 *Phys. Rev. Lett.* **82** 4951
- [27] Cohen D and Kottos T 2000 *Phys. Rev. Lett.* **85** 4839
- [28] Cohen D and Kottos T 2001 *Phys. Rev. E* **63** 36203